



Computational catalysis

A computational study of solution equilibria of platinum-based ethylene hydroamination catalytic species including solvation and counterion effects: Proper treatment of the free energy of solvation[☆]

Pavel A. Dub^{a,b}, Rinaldo Poli^{a,c,*}^a CNRS, LCC (Laboratoire de Chimie de Coordination), Université de Toulouse, UPS, INP, 205, route de Narbonne, F-31077 Toulouse, France^b A. N. Nesmeyanov Institute of Organoelement Compounds, Russian Academy of Sciences, Vavilov Street 26, 119991 Moscow, Russia^c Institut Universitaire de France, 103, bd Saint-Michel, 75005 Paris, France

ARTICLE INFO

Article history:

Available online 6 March 2010

Keywords:

Platinum
Catalytic hydroamination
Aniline complexes
Solvent models
DFT calculations
Counterion effect

ABSTRACT

A DFT/B3LYP study of the effect of the explicit inclusion of the Me₄P⁺ cation (as a model of nBu₄P⁺) on the calculation of solution equilibria involving anionic Pt^{II} complexes is reported. The calculated complexes are models of species that potentially participate in the low-energy portion of the catalytic cycle of the ethylene hydroamination by aniline catalyzed by the PtBr₂/(nBu₄P)Br system, namely (nBu₄P)₂[PtBr₄] (**1**), (nBu₄P)₂[Pt₂Br₆] (**1'**), (nBu₄P)[PtBr₃(C₂H₄)] (**2**), (nBu₄P)[PtBr₃(PhNH₂)] (**3**), *trans*-[PtBr₂(C₂H₄)(PhNH₂)] (**4**), *cis*-[PtBr₂(C₂H₄)(PhNH₂)] (**5**), *cis*-[PtBr₂(PhNH₂)₂] (**6**), *trans*-[PtBr₂(C₂H₄)₂] (**7**), and *cis*-[PtBr₂(C₂H₄)₂] (**8**). The relative energies are based on gas-phase geometry optimizations followed by C-PCM calculations of the solvation effects in dichloromethane and aniline at 25 °C and 150 °C. Three different approaches have been considered to describe the relative energies in solution: $\Delta E^{\text{CPCM}} (\Delta E_{\text{el}}^{\text{gas}} + \Delta \Delta G^{\text{solv}})$, $\Delta G_{\text{v}}^{\text{CPCM}} (\Delta E_{\text{el}}^{\text{gas}} + \Delta E_{\text{ZPVE}}^{\text{gas}} + \Delta E_{\text{v}}^{\text{gas}} - T\Delta S_{\text{v}}^{\text{gas}} + \Delta \Delta G^{\text{solv}})$ and $\Delta G^{\text{CPCM}} (\Delta H_{\text{gas}} - T\Delta S_{\text{gas}} + \Delta \Delta G^{\text{solv}})$, where $\Delta E_{\text{v}}^{\text{gas}}$ and $\Delta S_{\text{v}}^{\text{gas}}$ includes only the vibrational contribution and $\Delta \Delta G^{\text{solv}}$ for each compound is the solvation free energy resulting from the C-PCM calculation. The cation-anion association was found favourable in both solvents at the ΔE^{CPCM} and $\Delta G_{\text{v}}^{\text{CPCM}}$ levels, but nearly neutral at the ΔG^{CPCM} level. Consideration of the associated salts has a drastic effect on the energy scheme but significantly changes the relative energies only when doubly charged complexes are involved. The energy changes for equilibria that involve only neutral or singly charged species are not greatly affected by the cation inclusion. The ΔG^{CPCM} approach provides results in greater agreement with the available equilibrium data.

© 2010 Elsevier B.V. All rights reserved.

1. Introduction

Brunet and co-workers have unveiled in 2004 a simple and efficient catalyst – one of the most performing reported to date – for the intermolecular hydroamination of ethylene and higher olefins by anilines, which consists of ligandless PtBr₂ activated by nBu₄PBr [1–4]. A mechanism involving olefin activation followed by amine nucleophilic addition (as opposed to amine activation followed by olefin coordination and insertion) seems operative for this platinum catalyst [4] on the basis of a previous computational study on the [PtCl(C₂H₄)(PH₃)₂]⁺ model [5] and of the known stoichiometric reactivity of Pt-(olefin) complexes with amines [6–12]. However, the previous computational study addresses only models

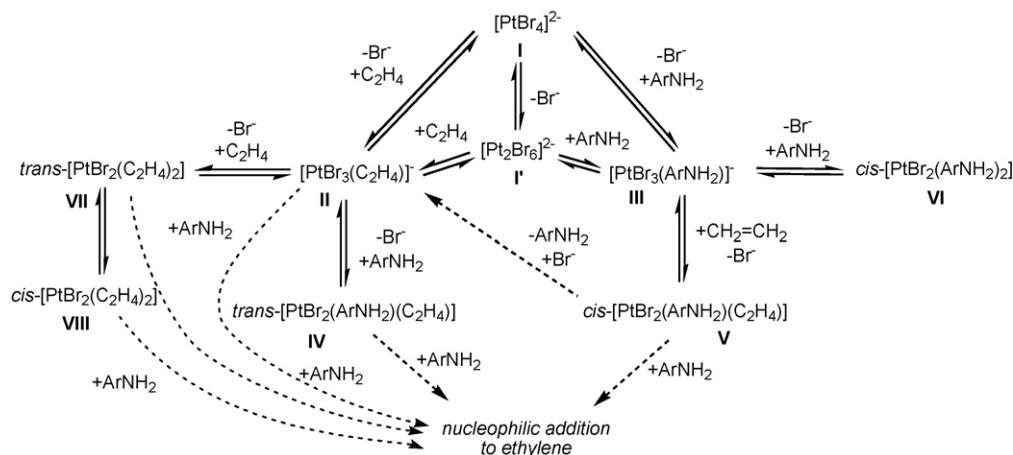
of phosphine-containing complexes, whereas the Brunet catalyst was found to be poisoned by phosphine ligands [1] while it is activated by halide anions (bromide being the best). Therefore, we set out to investigate the mechanistic details of this catalytic system both experimentally and computationally.

We have recently reported the synthesis and characterization of a variety of complexes formed by PtBr₂ in the presence of the activator (Br[−]) and substrates (ethylene, aniline) and a preliminary DFT investigation of their relative stability [13]. Thus, complexes (nBu₄P)₂[PtBr₄] (**1**), (nBu₄P)₂[Pt₂Br₆] (**1'**), (nBu₄P)[PtBr₃(C₂H₄)] (**2**), (nBu₄P)[PtBr₃(PhNH₂)] (**3**), *trans*-[PtBr₂(C₂H₄)(PhNH₂)] (**4**), *cis*-[PtBr₂(C₂H₄)(PhNH₂)] (**5**), and *cis*-[PtBr₂(PhNH₂)₂] (**6**) have been isolated and fully characterized. Complexes *trans*-[PtBr₂(C₂H₄)₂] (**7**) and *cis*-[PtBr₂(C₂H₄)₂] (**8**), although not synthesized, could also potentially be implicated as intermediates or off-loop catalytic species, since our preliminary DFT calculations show that they are energetically accessible by ligand exchange from [PtBr₃(C₂H₄)][−] and C₂H₄. It should also be mentioned that the related chlorido complexes, *cis* and *trans* [PtCl₂(C₂H₄)₂], have been reported by other authors [14–16].

[☆] This paper is part of a special issue on Computational Catalysis.

* Corresponding author at: CNRS, LCC (Laboratoire de Chimie de Coordination), Université de Toulouse, UPS, INP, 205, route de Narbonne, F-31077 Toulouse, France. Tel.: +33 561333173; fax: +33 561553003.

E-mail address: rinaldo.poli@lcc-toulouse.fr (R. Poli).



Scheme 1.

The experimental studies of the solution equilibria (in a variety of solvents at room temperature) backed up by the DFT study indicated that complex $[\text{PtBr}_3(\text{C}_2\text{H}_4)]^-$ is the most stable species and that all other complexes mentioned above are thermally accessible by simple ligand exchange. Scheme 1 shows the relationship between all these different complexes. A roman numeral is used to describe the complexes in solution, corresponding to the Arabic number of the isolated compounds. While this may seem redundant for the neutral compounds, it is important to distinguish the free complexes in solution from the isolated compounds in the case of charged species (e.g.: **I** is the $n\text{Bu}_4\text{P}^+$ salt of the dianion **I'**). All the ethylene containing complexes – **II**, **IV**, **V**, **VII** and **VIII** – are therefore potential candidates for aniline nucleophilic addition.

The above-mentioned theoretical calculations were performed without consideration of the counterion for the anionic species, using the B3LYP functional and applying the C-PCM model [17,18] on the gas-phase optimized geometries. The solution behaviour was described on the basis of the ΔG^{CPCM} parameter ($\Delta H^{\text{gas}} - T\Delta S^{\text{gas}} + \Delta\Delta G^{\text{solv}}$) [19], which gave results in qualitative agreement with the experimental equilibrium studies [13]. $\Delta\Delta G^{\text{solv}}$ is the difference between the solvation free energy corrective terms for the products and the reactants. There are questions, however, related to the partial quenching of translational and rotational modes, as well as the (*PV*) term, upon going from the gas phase to a condensed state. The problem of the accurate calculation of enthalpies and entropies in solution is a major computational challenge and no universal solution is apparently available [20–22]. A very common approach to the computational study of solution energetics involves the complete neglect of the gas-phase thermochemical parameters ($\Delta E^{\text{CPCM}} = \Delta E_{\text{el}}^{\text{gas}} + \Delta\Delta G^{\text{solv}}$), as this term is directly reported in the Gaussian output, but it should be noted that this approach mixes an electronic energy term with a free energy term and the result has no clear physical meaning. Another approach is based on the neglect of only the translational and rotational components of the gas-phase entropy term ($\Delta H^{\text{gas}} - T\Delta S_{\text{v}}^{\text{gas}} + \Delta\Delta G^{\text{solv}}$), where $\Delta S_{\text{v}}^{\text{gas}}$ represent the vibrational component of the entropy change for the system optimized in the gas phase [23]. Note, however, that this term has also no precise relevance, because if we assume complete quenching of the translational and rotational components of the molecular motions upon going from the gas phase to the solution, then the translational and rotational components of the overall partition function should be removed. That is, the translational and rotational contributions to the thermal energy should also be neglected, as well as the *PV* term, not only the translational and rotational contributions to the entropic term. Note that equalizing enthalpy and energy

in condensed phases is a common approximation. In this paper, we shall define a vibrational-only reaction free energy in solution, $\Delta G_{\text{v}}^{\text{CPCM}} = \Delta E_{\text{el}}^{\text{gas}} + \Delta E_{\text{ZPVE}}^{\text{gas}} + \Delta E_{\text{v}}^{\text{gas}} - T\Delta S_{\text{v}}^{\text{gas}} + \Delta\Delta G^{\text{solv}}$, where the gas-phase electronic energy term of the reaction, $\Delta E_{\text{el}}^{\text{gas}}$, is only corrected by the ZPVE term, $\Delta E_{\text{ZPVE}}^{\text{gas}}$, by the thermal vibrational contribution to the energy, $\Delta E_{\text{v}}^{\text{gas}}$, by the vibrational entropic contribution, $-T\Delta S_{\text{v}}^{\text{gas}}$, and by the solvation free energy corrective term, $\Delta\Delta G^{\text{solv}}$. A general problem is also the use of gas-phase frequencies for the calculation of the thermochemical parameters, because solution-phase optimizations are often haunted by several convergence problems. Another complication in our system, however, is the energetic effect of cation-anion association (ion pairing). Salts are generally present in solutions of low dielectric constant solvents as associated species, which may be energetically stabilized not only by Coulombic forces but also by specific non-covalent interactions (i.e. hydrogen bonds).

We have therefore wondered how the agreement of the above-mentioned different energy approaches (ΔE^{CPCM} , $\Delta G_{\text{v}}^{\text{CPCM}}$ and ΔG^{CPCM}) would change after inclusion of the counterion in the calculations. The present contribution reports new theoretical calculations (DFT/B3LYP) of the ionic complexes of Scheme 1 (**I**, **I'**, **II** and **III**) after inclusion of the cation, and new considerations on the agreement of the above-mentioned approaches to the description of the solution equilibria involving species **I–VIII**.

2. Computational methods

All geometry optimizations were performed with the Gaussian 03 suite of programs [24] using the B3LYP functional which includes the three-parameter gradient-corrected exchange functional of Becke [25] and the correlation functional of Lee, Yang, and Parr which includes both local and non-local terms [26,27]. In spite of several problems such as the underestimation of barrier heights, inaccuracy to describe weak interactions and overestimation of spin polarization, this functional was selected because it remains one of the most popular functionals used in transition metal computational chemistry [28]. In addition, all molecules described in this work are diamagnetic and the paramagnetic excited states are expected to be at much higher energy, thus the RHF description is appropriate. The basis set chosen was the standard 6–31+G*, which includes both polarization and diffuse functions that are necessary to allow angular and radial flexibility to the highly anionic systems, for all atoms of type H, C, N, P and Br. The Pt atom was described by the LANL2TZ(f) basis, which is an uncontracted version of LANL2DZ and includes an f polarization function and an ECP [29]. The starting geometries for

the calculations were those previously optimized for the free ion, after introduction of the cations at reasonable distances. Several relative positions of the cation and anion were used as input geometry in each case, and only the lower energy one in solution is reported (the others were generally very close in energy, typically at <1 kcal mol⁻¹ from the most stable structure). Stability tests carried out on several molecules with the Gaussian 03 default options showed stable wavefunctions in all cases. Frequency calculations were carried out for all optimized geometries in order to verify their nature as local minima and for the calculation of thermodynamic parameters at 298.15 K and at 423.15 K under the gas-phase and harmonic approximations. For the calculation of G_v^{CPCM} of each compound (equal to $E_{\text{el}}^{\text{gas}} + E_{\text{ZPVE}}^{\text{gas}} + E_v^{\text{gas}} - TS_v^{\text{gas}} + \Delta G_{\text{sol}}^{\text{CPCM}}$), the $(E_{\text{el}}^{\text{gas}} + E_{\text{ZPVE}}^{\text{gas}} + E_v^{\text{gas}})$ term was obtained as $[H^{\text{gas}}(T) - 4RT]$ or $[H^{\text{gas}}(T) - 2.5RT]$ for Br⁻, the corrective term consisting of 1.5RT for translation, 1.5RT for rotation (zero contribution to Br⁻), and RT for the PV term [30] whereas the S_v^{gas} term was read directly from the Gaussian output.

Solvent effects were included by means of C-PCM single point calculations on the gas-phase optimized geometries [17,18]. Among various continuum solvent models, the C-PCM was selected because of its generally better performance [31–33], even though there remains an inherent error when working with charged species [31]. The solvent cavity is created by a series of overlapping spheres by the default UA0 model and all standard settings as implemented in Gaussian 03 were used for the C-PCM calculations. Selected calculations have also been carried out with the IEF-PCM model [34–38] (see Results and Discussion section). The reaction free energy changes in solution were corrected for the change of standard state from the gas phase (1 atm) to solution (1 M) [39].

3. Results and discussion

3.1. Gas-phase geometries

Compounds **1**, **2** and **3** were modelled by simplifying the $n\text{Bu}_4\text{P}^+$ cation to the smaller PMe_4^+ (TMP), yielding systems (TMP)₂**I**, (TMP)**II** and (TMP)**III**. The dianion $[\text{Pt}_2\text{Br}_6]^{2-}$ (**I'**) does not participate in the catalytic cycle. However, it was experimentally found to result from the slow transformation (25 °C) of **I** in the absence of free bromide. Therefore, calculations on (TMP)₂**I'** were also carried out for comparison. For all the neutral complexes (**IV–VIII**) the geometries were already optimized in our previous study at the same level of theory [13].

The gas-phase optimized geometries of (TMP)₂**I**, (TMP)₂**I'**, (TMP)**II**, (TMP)**III**, and (TMP)Br are shown in Fig. 1. In general the addition of the cation does not significantly affect the geometry of the anionic complex, except for a minor Pt–Br bond shortening for **I**, **I'**, and the two Pt–Br bonds *trans* to each other in **II** and **III**, whereas the unique Pt–Br bond (*trans* to C₂H₄ in **II** and to PhNH₂ in **III**) slightly lengthens (comparisons are shown in SI). In addition, while free **I'** is planar, a slight bend across the Br_{br}···Br_{br} edge occurs for the geometry optimized in the presence of the two PMe_4^+ cations. This is certainly caused by the slightly asymmetric positioning of the two cations on the opposite sides of the dianion (see Fig. 1) and by the soft nature of the potential energy surface along this bending mode, as shown by the low frequencies of 13 and 33 cm⁻¹ where this molecular motion participates (vibrationally coupled with cation modes).

The cation–anion interactions are established through hydrogen bonds between the methyl C–H bonds as proton donors and the bromide anion or the bromido ligands for all the anionic complexes as proton acceptors. These are relatively weak interactions (the shortest H···Br distances are ca. 2.61 Å). For compounds (TMP)₂**I'** and (TMP)**III**, short interactions with the metal center (C–H···Pt) were also observed. A comparison of the normal modes

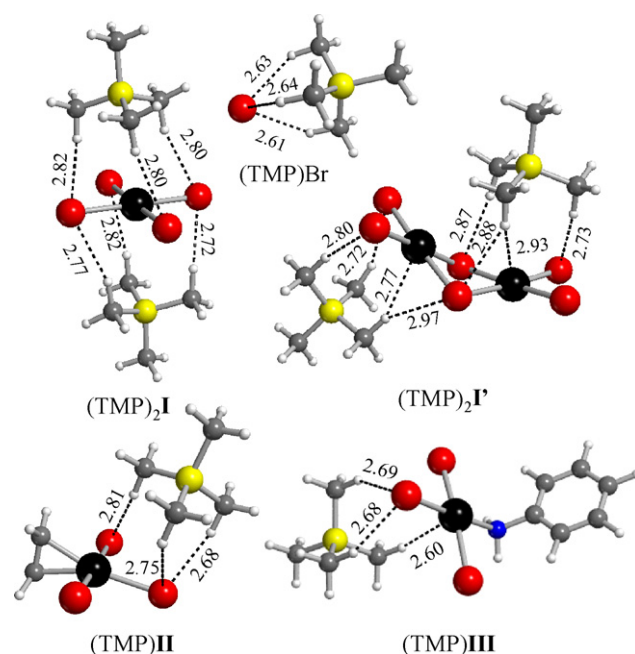


Fig. 1. Optimized geometries of the ion pairs used in this study. The closer cation–anion contacts are highlighted by dotted lines with the distances reported in Å.

in the presence and absence of the cation reveals a correlation between the frequency shift and the bond length changes, with the greater shift (18 cm⁻¹ to higher frequency) being observed for the E_u out-of-phase Br–Pt–Br stretching vibration in **I**. Certain Pt–Br stretching modes also reveal vibrational coupling with the cation vibrations. The cation effect on the calculated frequencies has also been analyzed in a recent contribution for the $\text{Me}_3\text{SiO}^- \text{K}^+$ salt [40]. The extrapolation of these results to the real $n\text{Bu}_4\text{P}^+$ salts clearly involves approximations related to the steric and inductive effects of the $n\text{Bu}$ group and to the possibility that other C–H bonds of the $n\text{Bu}$ chains also participate in the cation–anion interactions. It is likely that the $n\text{Bu}_4\text{P}^+$ cation also interacts with the anion through the α C–H bonds, since these should have the greater acidic character being closer to the positively charged P atom.

3.2. Ion pairing energies

Since the equilibrium studies reported in our previous contribution [13] were carried out in dichloromethane at room temperature, the C-PCM calculations were also carried out in this solvent, as single point calculations on the gas-phase optimized geometries. An approximation is related to use of this procedure, since the best geometry could in principle change upon going from the gas phase to a condensed phase. However, a recent test carried out in our group for ion pairs of type $[\text{Cp}^*\text{Mo}(\text{PMe}_3)_2(\text{CO})\text{H}_2]^+[\text{BF}_4]^-$ has shown insignificant changes when the geometry was reoptimized with the C-PCM in either THF or dichloromethane. The internal geometries of the ions were practically unaffected, whereas the cation–anion interactions became slightly looser, but the effect on the energy was in each case below 0.2 kcal mol⁻¹ relative to the corresponding fixed-point C-PCM calculations on the gas-phase optimized geometries [41]. Considering also the convergence problems that are frequently associated with the geometry optimizations in the presence of a C-PCM, we opted to use only the gas-phase optimized geometries. The thermal and entropy corrections to the gas-phase electronic energies were done at 298.15 K to allow comparison with the experiment. C-PCM calculations were also run in aniline at 298.15 K and at 423.15 K. These cannot be

Table 1
Solvation free energies for selected species in CH₂Cl₂ at 298.15 K under different continuum model approaches.

Species	$\Delta G_{\text{sol}}^{\text{CPCM}}$ (kcal mol ⁻¹)	$\Delta G_{\text{sol}}^{\text{IEFPCM}}$ (kcal mol ⁻¹)
PMe ₄ ⁺	-37.16	-36.88
C ₂ H ₄	1.79	1.88
PMe ₄ ⁺ Br ⁻	-16.25	-15.21
Br ⁻	-58.93	-58.93
[PtBr ₃ (C ₂ H ₄)] ⁻	-39.51	-39.01
[PtBr ₄] ²⁻	-149.52	-148.97

compared with experimental results, but are useful for prediction purposes because the catalytic experiments are run in aniline at 150 °C. Therefore, they are only provided in the Supporting Information. Calculations of solvation free energies on specific neutral, cationic and anionic species were also carried out with the IEF-PCM model (see Table 1). These showed very small changes, <0.5 kcal mol⁻¹ in most cases, with the notable exception of the PMe₄⁺Br⁻ ion pair (difference of ca. 1 kcal mol⁻¹). The combination of these solvation energy changes for reactants and products in the ion pairing (Eq. (1)) and ligand exchange (Eq. (7)) processes described later yields only minimal energy effects (<1 kcal mol⁻¹ under all three approaches, ΔE^{CPCM} , $\Delta G_{\text{v}}^{\text{CPCM}}$ or ΔG^{CPCM}).

It is first useful to analyze the outcome of the three different approaches to describe the energetic of the ion pair formation. The processes of interest are outlined in Eqs. (1)–(5) and the results are reported in Table 2. The ΔE^{CPCM} data show that the association is more favourable as expected for the 2:1 salts than for the 1:1 salts. This trend remains valid at the $\Delta G_{\text{v}}^{\text{CPCM}}$ level. A more detailed analysis reveals an interesting trend. On going from ΔE^{CPCM} to $\Delta G_{\text{v}}^{\text{CPCM}}$, the difference between them being the $\Delta(E_{\text{ZPVE}}^{\text{gas}} + E_{\text{v}}^{\text{gas}} - TS_{\text{v}}^{\text{gas}})$ term, the change is very small for the Br⁻ system (-1.2 kcal mol⁻¹), intermediate for the other 1:1 salts (-5.5 kcal mol⁻¹ for **II** and -4.8 kcal mol⁻¹ for **III**) and greater for the 2:1 salts (-9.8 kcal mol⁻¹ for **I** and -12.5 kcal mol⁻¹ for **I'**). The major cause for this trend is the difference of the $\Delta S_{\text{v}}^{\text{gas}}$ term, which is also reported for convenience in Table 2. All the $\Delta S_{\text{v}}^{\text{gas}}$ terms are positive, because a number of new low-frequency vibrational modes in the product (related to the relative movement of the cation and anion with respect to each other) are generated from translational and rotational modes in the reagents. For the bromide salt, the separated ions have nine translational and rotational modes (no rotational modes for the spherical Br⁻ ion), thus only three new vibrational modes are generated in the ion pair. For the salts of **II** and **III**, both separate ions have six non-vibrational modes, thus six new vibrational modes result in the product. Finally, for the 2:1 salts of **I** and **I'**, the product contains 12 additional vibrational modes relative to the separate ions. Indeed, the value of $\Delta S_{\text{v}}^{\text{gas}}$ is roughly proportional to the number of new vibrational modes. The actual values are of course determined by the frequencies of the new vibrational modes, as well as from the frequency changes in the other modes.

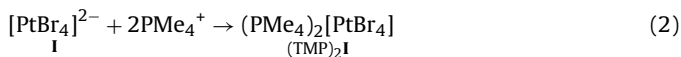
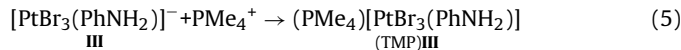
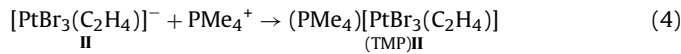
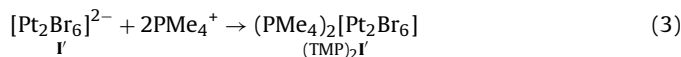


Table 2
Relative energies changes for the ion pair formations at 298.15 K in dichloromethane.

Anionic system	ΔE^{CPCM} (kcal/mol)	$\Delta G_{\text{v}}^{\text{CPCM}}$ (kcal/mol)	ΔG^{CPCM} (kcal/mol)	$\Delta S_{\text{v}}^{\text{gas}}$ (e.u.)
Br ⁻ (Eq. (1))	-10.0	-11.2	-2.5	8.8
I (Eq. (2))	-28.3	-38.1	-5.9	53.2
I' (Eq. (3))	-22.1	-34.6	-0.7	65.3
II (Eq. (4))	-9.1	-14.6	1.5	30.4
III (Eq. (5))	-9.5	-14.3	2.4	28.2



On going from $\Delta G_{\text{v}}^{\text{CPCM}}$ to ΔG^{CPCM} , on the other hand, the association becomes nearly ergoneutral for all salts. The major difference between these two parameters corresponds to the $\Delta(-TS_{\text{trans}}^{\text{gas}} - TS_{\text{rot}}^{\text{gas}})$ term, which is much greater for the 2:1 salts (8.7, Br⁻; 16.1, **II**; 16.7, **III**; 32.2, **I**; 33.9, **I'**; all values are in kcal mol⁻¹), plus a smaller term due to $\Delta(E_{\text{tr}}^{\text{gas}} + E_{\text{rot}}^{\text{gas}} + PV)$. This trend is related to the loss of a greater number of translational and rotational modes in the order Br⁻ (3) < **II**, **III** (6) < **I**, **I'** (12).

The question now revolves around which approach yields results in better agreement with the experiment. We do not have quantitative values for the experimental association constants of these salts in dichloromethane, but values for similar salts are available in the literature. For simple bromide salts in dichloromethane, relevant values are $2.5(2) \times 10^4$ for nBu₄NBr [42], $6.6(1) \times 10^4$ [42] or $8.0(5) \times 10^4$ [43] for Et₄NBr, 3.9×10^3 for Ph₄AsBr [44] and 1.2×10^3 for [PPN]Br [42]. Note the cation dependence, the values of the ammonium salts being greater than those of the bulkier Ph₄As⁺ and PPN⁺ salts. We can predict intermediate values for the nBu₄P⁺ salt, i.e. $\sim 10^4$. For 1:1 salts of similar size to **2** and **3**, relevant values in dichloromethane are 1.94×10^4 for Et₄N[FeBr₄] [45], 4.25×10^3 for Ph₄As[FeBr₄] [45], 6.8×10^4 and 1.8×10^4 for the PF₆⁻ and BPh₄⁻ salts of [Pt(tmda)(Me₂SO)Cl]⁺ [46], and $3.8(3) \times 10^3$ for [Cp*₂Fe]PF₆. The association constants for the nBu₄P⁺ salts of **II** and **III** could also be reasonably estimated as being greater than 10³. We could not find data for 2:1 salts in dichloromethane. For equilibrium constants of 10³ and 10⁴ at 298 K, the corresponding ΔG°_{298} is -5.5 and -4.1 kcal mol⁻¹, respectively.

Comparison between these ΔG values and the results in Table 2 shows that, as could be expected, the anticipated experimental results lay in-between the ΔG^{CPCM} and $\Delta G_{\text{v}}^{\text{CPCM}}$ values. In other words, a full gas-phase entropy correction overshoots the solution ΔG value. On the other hand, because of the above discussed transformation of translational and rotational modes into vibrational modes, the vibrational entropy term ($-T\Delta S_{\text{v}}$) yields a negative correction for this particular ion association process, thus the ΔE^{CPCM} values are placed in-between the $\Delta G_{\text{v}}^{\text{CPCM}}$ and ΔG^{CPCM} values for all salts. These ΔE^{CPCM} values appear to be in closer agreement with the expected experimental values than the values of either the $\Delta G_{\text{v}}^{\text{CPCM}}$ of the ΔG^{CPCM} approach, at least for the 1:1 salts (TMP)**II** and (TMP)**III**. Therefore, use of ΔE^{CPCM} values for the evaluation of ion pairing equilibria, at least for 1:1 salts, should not give results far off reality in general.

3.3. Application to the solution equilibria

The relative ΔG^{CPCM} values for species **I–VIII** were already reported and discussed in our previous contribution [13], but no analysis of the corresponding ΔE^{CPCM} and $\Delta G_{\text{v}}^{\text{CPCM}}$ was offered. For this reason, the complete set of values for these species accord-

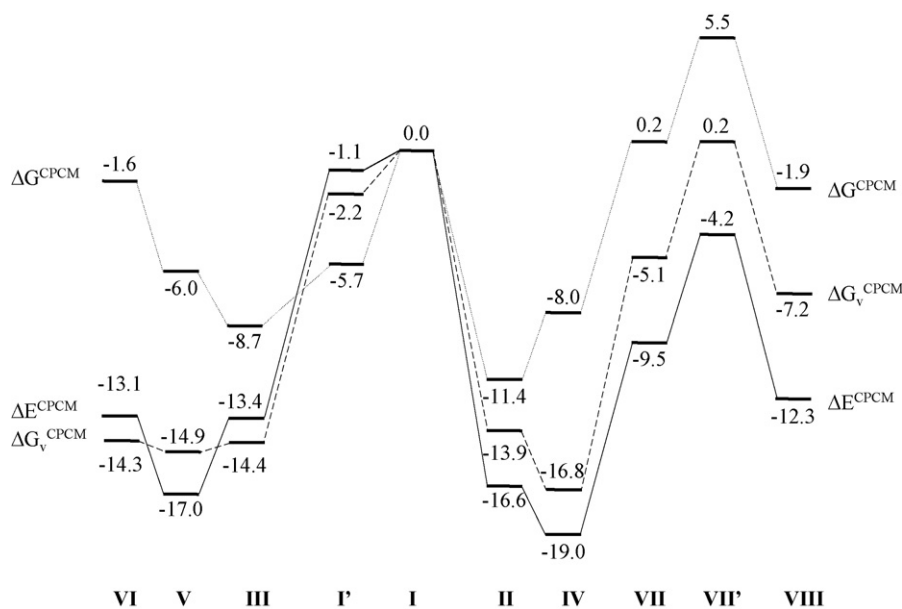
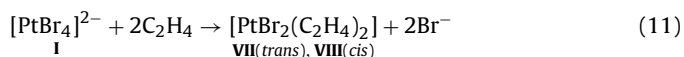
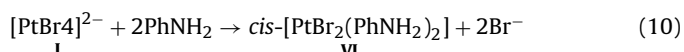
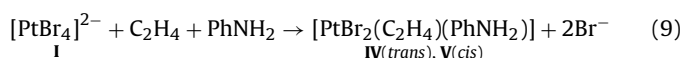
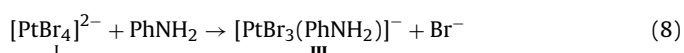
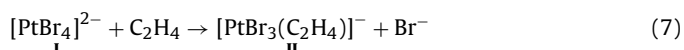
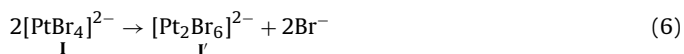


Fig. 2. Energy diagram for the ΔE^{CPCM} (plain lines), ΔG_v^{CPCM} (dashed lines), and ΔG^{CPCM} (dotted lines) approaches for the anionic model in dichloromethane at 25 °C. All values are reported in kcal mol⁻¹ relative to I. Species VII' is a different conformer of VII, where one C₂H₄ ligand has the C–C axis coplanar with the coordination plane [13].

ing to the three models is given in Fig. 2 for the dichloromethane solution. The calculation of the energy value in each case takes into account all species consumed and produced starting from the reference system I, as outlined in Eqs. (6)–(11). The corresponding diagrams in aniline at 25° and 150 °C are presented in SI. The data are presented according to the synthetic strategy. Starting from I and I' in the center, addition of ethylene or aniline leads to II (right) and III (left). Then, complex IV, VII and VIII, shown further on the right, are obtained or can be imagined to result from the addition of aniline or ethylene to II, whereas complexes V and VI, further to the left of I, are obtained by addition of ethylene or aniline to complex III.



For all complexes, except for I', $\Delta G^{\text{CPCM}} > \Delta G_v^{\text{CPCM}}$ and generally $\Delta G_v^{\text{CPCM}} > \Delta E^{\text{CPCM}}$ (except for I', III and VI). The ΔG_v^{CPCM} and ΔE^{CPCM} values are relatively close to each other, whereas ΔG^{CPCM} is significantly greater. This reflects the fact that, for most of the Eqs. (6)–(11), ΔS_v^{gas} and $\Delta(S_{\text{trans}}^{\text{gas}} + S_{\text{rot}}^{\text{gas}})$ are negative and the former is smaller than the latter. The $\Delta(E_{\text{tr}}^{\text{gas}} + E_{\text{rot}}^{\text{gas}} + PV)$ term gives a zero contribution to all reactions with equal number of species on the reactants and products sides, and the ΔE_v^{gas} term is small. Eq. (6), where the molecularity increases, is the only one where both $\Delta(S_{\text{trans}}^{\text{gas}} + S_{\text{rot}}^{\text{gas}})$ and ΔS_v^{gas} are positive. The same trends are observed in aniline (see SI). The lowest energy species is complex IV according to the ΔE^{CPCM} and ΔG_v^{CPCM} approaches, while complex II is most stable within the ΔG^{CPCM} approach.

The energies differences between different neutral compounds are not affected by the presence of the counterion. Hence, they can

already be analyzed on the basis of the results in Fig. 2. For instance, for the mixed-ligand system $[\text{PtBr}_2(\text{C}_2\text{H}_4)(\text{PhNH}_2)]$ the *trans* isomer has a lower energy than the *cis* (IV < V) by 2.0 kcal mol⁻¹ for all energy models. This agrees with the experimental evidence reported in our previous contribution [13]. On the other hand, the *cis* isomer has a lower energy than the *trans* for the $\text{PtBr}_2(\text{C}_2\text{H}_4)_2$ system (VIII < VII; 2–3 kcal mol⁻¹ depending on the energy model). This is consistent with the experimental evidence reported for the related dichloride system [15,16]. The neutral ligand exchange processes leading from the mixed-ligand complexes $[\text{PtBr}_2(\text{C}_2\text{H}_4)(\text{PhNH}_2)]$ (IV and V) to the dianiline (VI) or diethylene (VII and VIII) complexes are unfavourable for all energy models. This is again consistent with the experimental evidence, since addition of ethylene to III stops at V and addition of aniline to II stops at IV. As it can be appreciated, solvation entropy plays a very minor role in these equilibria between neutral species, because the same number of molecules appears on each side. Hence, all approaches reproduce equally well the experiment.

Combination of the ion pairing energies of Table 2 with the relative energies shown in Fig. 2 for the solution equilibria of Eqs. (6)–(11) yields the results summarised in Fig. 3 for dichloromethane at 25 °C, where the system used as reference is (TMP)₂I. The same schemes in aniline solution at 25 °C and 150 °C are presented in SI. The processes leading to the species of interest are the same ones already outlined in Eqs. (6)–(11), but with all charged species in the associated form with the PMe_4^+ cation.

The association of the ionic complexes with the PMe_4^+ cation has a drastic effect on the energy scheme, cf. Figs. 2 and 3. The ion association process (see Table 2) has the effect of stabilizing all charged species, but the more highly charged species benefit from a greater stabilization. The three monoanionic species (complexes II and III and the Br⁻ ion) are stabilized by approximately the same amount, especially at the ΔE^{CPCM} level, whereas the stabilization of the dianionic complexes is worth more than twice as much on the ΔE^{CPCM} and ΔG_v^{CPCM} scales. Therefore, the energy values for all equilibria relating a monoanionic complex with a neutral complex (with release of a Br⁻ ion) are not affected very much, whereas the equilibria relating the doubly charged species I with the singly charged species II and III or with the neutral species are strongly affected by ion pairing at the ΔE^{CPCM} and ΔG_v^{CPCM} levels. On the other hand, the picture changes relatively little at the ΔG^{CPCM} level because the

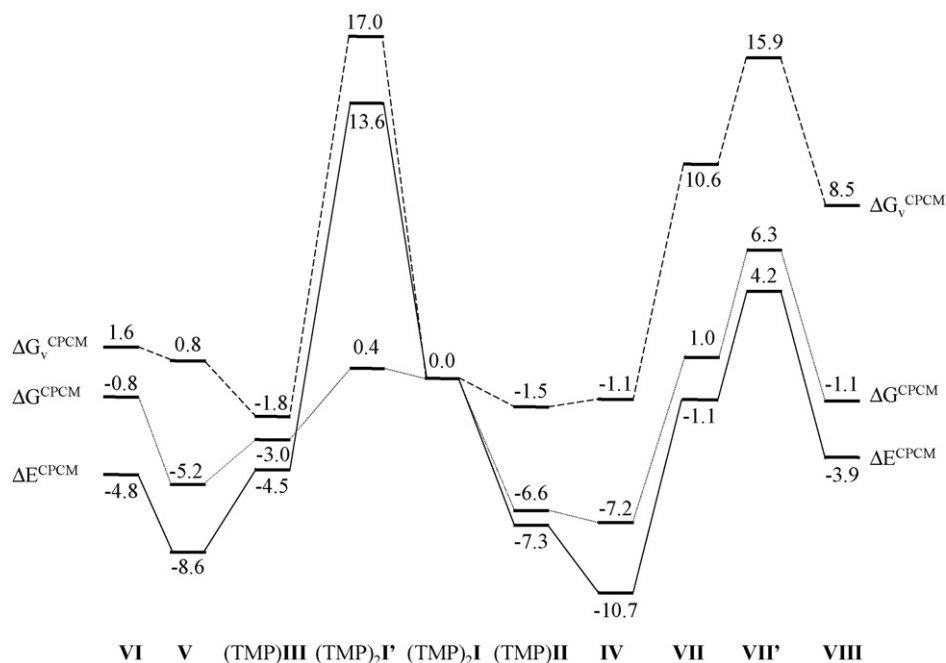
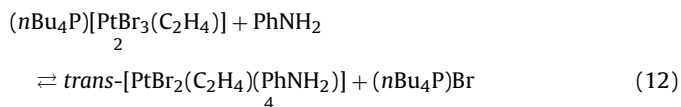


Fig. 3. Energy diagram for the ΔE^{CPCM} (plain lines), ΔG_v^{CPCM} (dashed lines), and ΔG^{CPCM} (dotted lines) approaches for the neutral model in dichloromethane at 25 °C. All values are reported in kcal mol⁻¹ relative to (TMP)₂I.

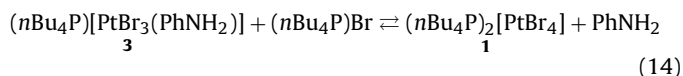
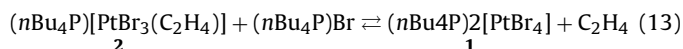
ΔG^{CPCM} values of all ion association equilibria (Table 2) are close to zero. Hence, the relative stabilization of all compounds (except I') relative to I are greatly reduced on the ΔE^{CPCM} and ΔG_v^{CPCM} scales but not as much on the ΔG^{CPCM} scale (cf. Figs. 2 and 3) and consequently ΔG_v^{CPCM} ≫ ΔG^{CPCM} > ΔE^{CPCM} for all compounds, except I', relative to compound (TMP)₂I. The process leading from (TMP)₂I to (TMP)₂I' transforms two doubly charged species to a new dianionic species and two monoanionic ones. The result is a great destabilization on the ΔE^{CPCM} and ΔG_v^{CPCM} scales.

The ion pair model of Fig. 3 entails small qualitative changes relative to the free ion model of Fig. 2 concerning the nature of the most stable species in solution: the ΔG^{CPCM} approach now suggests a greater stability for complex IV, whereas it favoured II under the free ion model, while the ΔG_v^{CPCM} approach now slightly favours (TMP)II, whereas it favoured IV under the free ion model. However, the difference between (TMP)II and IV is only 0.6 kcal/mol in favour of the latter (ΔG^{CPCM}) or 0.4 kcal/mol in favour of the former (ΔG_v^{CPCM}). Recall that the experimental studies indicate a greater thermodynamic stability for compound 2 (equilibrium 12 is largely shifted to the left). This result would seem better reproduced by the ΔG_v^{CPCM} approach for the neutral model and by the ΔG^{CPCM} approach for the ionic model.

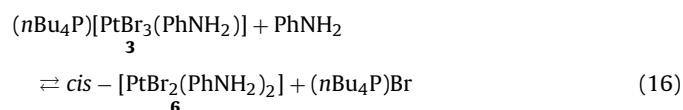
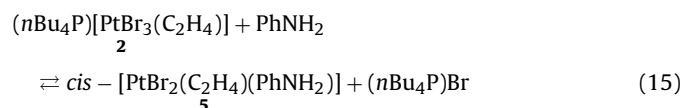


It is also useful to recall the other experimental results [13] relating ionic and neutral species, or ionic species of different charge, and compare them with the computational results in Figs. 2 and 3. Compound 2 is stable relative to 1 in the presence of excess (nBu₄P)Br, but a certain amount of 1 was generated unless a protected atmosphere of ethylene was present. This suggests that equilibrium 13 is largely shifted to the left hand side, but the free energy difference cannot be more than a few kcal mol⁻¹. Similarly, equilibrium 14 is also largely shifted toward the left hand side because addition of excess (nBu₄P)Br to 3 resulted in only minor transformation to 1. It is difficult to make estimations because the

experimental evidence was only qualitative with no accurate determination of the equilibrium concentrations. However, the large stabilization predicted for II and III relative to I by the ionic model (Fig. 2) should lead to no significant formation of 1 from either 2 or 3 under essentially any conditions. The energy differences shown in Fig. 3 seem more reasonable, confirming the importance of the cation–anion associations in the energy calculations.

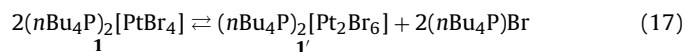


Equilibrium 15 between compounds 2 and 5 was found displaced toward the left hand side, although the conversion of 5 to 2 in the presence of a slightly substoichiometric amount of (nBu₄P)Br did not lead to complete bromide consumption [13] (this study was carried out in DFM due to the insolubility of 5 in dichloromethane). Equilibrium 16 between compounds 3 and 6 was also found displaced toward the left hand side, in this case with apparent quantitative conversion of 6 to 3. These results are consistent for the ionic model only under the ΔG^{CPCM} approach, whereas the neutral model predicts the correct result for both equilibria under both approaches (ΔG^{CPCM} and ΔG_v^{CPCM}).



Finally, equilibrium 17 appears displaced toward the left but not by a large amount, because a small amount of 1' was spontaneously generated upon prolonged standing from dichloromethane

solutions of **1** in the absence of free bromide. As shown in Fig. 2, the free ion model would predict an essentially quantitative conversion of **1** to **1'**, whereas the ion pair model of Fig. 3 can be reconciled with the experiment, under the logical assumption of a partial quenching of the translational and rotational components of the reaction entropy.



In summary, the utility of the associated salt model is evident for the description of the equilibria involving highly charged species. When only monocharged species are involved, roughly speaking, both the free ion and the ion pair models describe the solution equilibria with acceptable accuracy, but only when the thermochemical parameters (PV and $-TS$) are introduced to some degree. The ΔE^{CPCM} approach, although apparently the best one to describe the ion association equilibria, does not yield results in agreement with experiment for the ligand exchange equilibria (except for the equilibria relating neutral species). Concerning the best approach for handling the solution entropy problem, conventional wisdom suggests that the real solution must lay in-between the ΔG^{CPCM} and ΔG_v^{CPCM} solutions and the qualitative comparison of the computational results according to the ion pair model with the available equilibria shows that this indeed the case. At a very qualitative level, it seems that the experimental result lies closer to the ΔG^{CPCM} prediction than to the ΔG_v^{CPCM} prediction for equilibria involving large changes in charge localization (ion associations for 1:1 salts in Table 2 and equilibrium 17). This amounts to saying that there is no significant quenching of the translational and rotational modes of the various compounds on going from the gas phase to the dichloromethane solution. Otherwise stated, these modes are transformed to very active (low frequency) librations in the solvent cage, greatly contributing to the free energy of the system.

It is not possible to exclude, however, that the shortcoming of various approximations used in the computations lead to systematic errors in favour of ΔG^{CPCM} approach. Amongst these approximations, we can mention the inaccuracy of the harmonic approximation, use of Me_4P^+ as a model of $n\text{Bu}_4\text{P}^+$, use of gas-phase optimized rather than solution-phase optimized geometries, and the nature of the functional. However, one additional approximation that might turn out to affect significantly the quality of the calculations is the total neglect of specific interactions (notably hydrogen bonding) between the reagents participating in the considered equilibria with each other and with solvent molecules. For instance, the free aniline and the aniline ligand coordinated to **III** in equilibrium (8) can serve as proton donors in hydrogen bonding with the bromido ligands of **I** and **III** and with the free bromide ion. Similar effects would operate on equilibria 9 and 10.

As a final remark, the investigation of the platinum-catalyzed hydroamination by aniline potentially involves several platinum complexes as intermediates and off-loop species, some of which may be neutral, others anionic. Insofar as these species have a single negative charge, the use of the ionic model seems to provide relevant results, while the participation of doubly charged anions may require a more elaborate study using the associated species. It should be mentioned that other theoretical studies have reported the need to include the counterion. Most typically, the counterion in these previous contributions interacts with the catalytic system by coordinating the metal (e.g. F^- or Cl^-) [47,48] or assists intramolecular rearrangement steps (e.g. proton transfer by TfO^- [49]) and thus changes the nature of the catalytic resting state and/or transition state of the rate determining step. Great attention has been devoted to the control of the structure and relative stability of dormant species and transition states in polymerization catalysis [50–61], while other studies address the orientation or steric influence of the counterion for other types of potential catalytic sites

[62–64]. In our case, the $n\text{Bu}_4\text{P}^+$ cation should in principle not play any role other than ion pairing. The explicit effect of the counterion on the relative energetics through cation–anion association equilibria in relation with catalytic processes does not appear to be systematically investigated.

4. Conclusions

The availability of solution equilibrium information relating neutral and charged Pt^{II} complexes (precatalysts, intermediates or off-loop species for the ethylene hydroamination by aniline) has given us the opportunity to test the accuracy of various energy approaches within the C-PCM model for their description. Consideration of the cation–anion association in the low permittivity dichloromethane and aniline solvents has drastic effect on the energy scheme in comparison to the free ion model, although practically no effect is observed on the geometries and frequencies of the anionic complexes. Consideration of ion pairing is essential for equilibria involving highly charged anionic complexes (<-1), whereas those implicating only neutral and singly charged species are described reasonably well by both the free ion and ion pair models. The most important point is the inadequacy of the common ΔE^{CPCM} ($\Delta E_{\text{el}}^{\text{gas}} + \Delta \Delta G_{\text{Solv}}$) approach, whereas models that introduce the gas-phase thermodynamic parameters, ΔG_v^{CPCM} and ΔG^{CPCM} , provide results in better agreement with the experimental results. However, the ΔE^{CPCM} gives better estimates for the solution free energy of the ion pairing process. The correct handling of the solute translational and rotational partition function for accurate calculation of solution equilibrium positions is one of the outstanding challenges for computational chemistry. The additional complication of ion pairing equilibria adds another dimension to the complexity of the calculation, but the present contribution shows that relatively significant results can be obtained. We believe that extensive benchmarking using simple ion pairing equilibria that are experimentally well determined at the quantitative level can be of great help for the analysis of the partially quenched translational and rotational motions of solutes.

In terms of our exploration of the Pt^{II} -catalyzed hydroamination mechanism and more specifically the investigation of the high-energy portion of the catalytic cycle, the results presented in the present contribution will be of guidance for the selection of the most suitable computational approach. This investigation is currently ongoing and the results will be reported in due course.

Acknowledgement

We thank the CNRS and the RFBR for support through a France-Russia (RFBR-CNRS) bilateral grant No. 08-03-92506, and the MENESR (Ministère de l'Éducation nationale de l'enseignement supérieur et de la recherche de France) for the Ph.D. fellowship to P.A.D.

Appendix A. Supplementary data

Supplementary data associated with this article can be found, in the online version, at [doi:10.1016/j.molcata.2010.03.003](https://doi.org/10.1016/j.molcata.2010.03.003).

References

- [1] J.J. Brunet, M. Cadena, N.C. Chu, O. Diallo, K. Jacob, E. Mothes, *Organometallics* 23 (2004) 1264–1268.
- [2] J.J. Brunet, N.C. Chu, O. Diallo, *Organometallics* 24 (2005) 3104–3110.
- [3] M. Rodriguez-Zubiri, S. Anguille, J.-J. Brunet, *J. Mol. Catal. A* 271 (2007) 145–150.
- [4] J.-J. Brunet, N.-C. Chu, M. Rodriguez-Zubiri, *Eur. J. Inorg. Chem.* (2007) 4711–4722.
- [5] H.M. Senn, P.E. Blochl, A. Togni, *J. Am. Chem. Soc.* 122 (2000) 4098–4107.
- [6] R. Palumbo, A. De Renzi, A. Panunzi, G. Paiaro, *J. Am. Chem. Soc.* 91 (1969) 3874–3879.

- [7] A. Panunzi, A. De Renzi, R. Palumbo, G. Paiaro, *J. Am. Chem. Soc.* 91 (1969) 3879–3883.
- [8] A. Panunzi, A. Derenzi, G. Paiaro, *J. Am. Chem. Soc.* 92 (1970) 3488–3489.
- [9] E. Benedetti, A. De Renzi, G. Paiaro, A. Panunzi, C. Pedone, *Gazz. Chim. Ital.* 102 (1972) 744–754.
- [10] D. Hollings, M. Green, D.V. Claridge, *J. Organometal. Chem.* 54 (1973) 399–402.
- [11] T.E. Muller, M. Beller, *Chem. Rev.* 98 (1998) 675–703.
- [12] T.E. Müller, K.C. Hultsch, M. Yus, F. Foubelo, M. Tada, *Chem. Rev.* 108 (2008) 3795–3892.
- [13] P.A. Dub, M. Rodriguez-Zubiri, J.-C. Daran, J.-J. Brunet, R. Poli, *Organometallics* 28 (2009) 4764–4777.
- [14] J. Chatt, R.G. Wilkins, *Nature (Lond., UK)* 165 (1950) 859–860.
- [15] M.R. Plutino, S. Otto, A. Roodt, L.I. Elding, *Inorg. Chem.* 38 (1999) 1233–1238.
- [16] S. Otto, A. Roodt, L.I. Elding, *Inorg. Chem. Commun.* 9 (2006) 764–766.
- [17] V. Barone, M. Cossi, *J. Phys. Chem. A* 102 (1998) 1995–2001.
- [18] M. Cossi, N. Rega, G. Scalmani, V. Barone, *J. Comput. Chem.* 24 (2003) 669–681.
- [19] A.A.C. Braga, G. Ujaque, F. Maseras, *Organometallics* 25 (2006) 3647–3658.
- [20] C.E. Chang, W. Chen, M.K. Gilson, *J. Chem. Theory Comput.* 1 (2001) 1017–1028.
- [21] J. Carlsson, J. Aqvist, *J. Phys. Chem. B* 109 (2005) 6448–6456.
- [22] N. Singh, A. Warshel, *J. Phys. Chem. B* 113 (2009) 7372–7382.
- [23] M. Sumimoto, N. Iwane, T. Takahama, S. Sakaki, *J. Am. Chem. Soc.* 126 (2004) 10457–10471.
- [24] G.W.T.M.J. Frisch, H.B. Schlegel, G.E. Scuseria, M.A. Robb, J.R. Cheeseman, J.A. Montgomery, T. Vreven, K.N. Kudin, J.C. Burant, J.M. Millam, S.S. Iyengar, J. Tomasi, V. Barone, B. Mennucci, M. Cossi, G. Scalmani, N. Rega, G.A. Petersson, H. Nakatsuji, M. Hada, M. Ehara, K. Toyota, R. Fukuda, J. Hasegawa, M. Ishida, T. Nakajima, Y. Honda, O. Kitao, H. Nakai, M. Klene, X. Li, J.E. Knox, H.P. Hratchian, J.B. Cross, C. Adamo, J. Jaramillo, R. Gomperts, R.E. Stratmann, O. Yazyev, A.J. Austin, R. Cammi, C. Pomelli, J.W. Ochterski, P.Y. Ayala, K. Morokuma, G.A. Voth, P. Salvador, J.J. Dannenberg, V.G. Zakrzewski, S. Dapprich, A.D. Daniels, M.C. Strain, O. Farkas, D.K. Malick, A.D. Rabuck, K. Raghavachari, J.B. Foresman, J.V. Ortiz, Q. Cui, A.G. Baboul, S. Clifford, J. Cioslowski, B.B. Stefanov, G. Liu, A. Liashenko, P. Piskorz, I. Komaromi, R.L. Martin, D.J. Fox, T. Keith, M.A. Al-Laham, C.Y. Peng, A. Nanayakkara, M. Challacombe, P.M.W. Gill, B. Johnson, W. Chen, M.W. Wong, C. Gonzalez, J.A. Pople, *Gaussian 03, Revision C. 02*, Gaussian, Inc., Wallingford, CT, 2004.
- [25] A.D. Becke, *J. Chem. Phys.* 98 (1993) 5648–5652.
- [26] C.T. Lee, W.T. Yang, R.G. Parr, *Phys. Rev. B* 37 (1988) 785–789.
- [27] B. Miehlich, A. Savin, H. Stoll, H. Preuss, *Chem. Phys. Lett.* 157 (1989) 200–206.
- [28] Y. Zhao, D.G. Truhlar, *Acc. Chem. Res.* 41 (2008) 157–167.
- [29] L.E. Roy, P.J. Hay, R.L. Martin, *J. Chem. Theory Comput.* 4 (2008) 1029–1031.
- [30] J.W. Ochterski, http://www.gaussian.com/g_whitepap/thermo.htm (2000).
- [31] Y. Takano, K.N. Houk, *J. Chem. Theory Comput.* 1 (2005) 70–77.
- [32] A. Klamt, B. Mennucci, J. Tomasi, V. Barone, C. Curutchet, M. Orozco, F.J. Luque, *Acc. Chem. Res.* 42 (2009) 489–492.
- [33] J.M. Ho, M.L. Coote, *Theor. Chem. Acc.* 125 (2010) 3–21.
- [34] E. Cancès, B. Mennucci, J. Tomasi, *J. Chem. Phys.* 107 (1997) 3032–3041.
- [35] B. Mennucci, J. Tomasi, *J. Chem. Phys.* 106 (1997) 5151–5158.
- [36] B. Mennucci, E. Cancès, J. Tomasi, *J. Phys. Chem. B* 101 (1997) 10506–10517.
- [37] M. Cossi, V. Barone, B. Mennucci, J. Tomasi, *Chem. Phys. Lett.* 286 (1998) 253–260.
- [38] J. Tomasi, B. Mennucci, E. Cancès, *J. Mol. Struct. Theochem.* 464 (1999) 211–226.
- [39] P. Winget, C.J. Cramer, D.G. Truhlar, *Theor. Chem. Acc.* 112 (2004) 217–227.
- [40] M. Montejo, F.P. Urena, F. Marquez, A.M. Ingrain, J.L. Gonzalez, *J. Raman Spectrosc.* 39 (2008) 460–467.
- [41] P.A. Dub, N.V. Belkova, O.A. Filippov, J.-C. Daran, L.M. Epstein, A. Lledós, E.S. Shubina, R. Poli, *Chem. Eur. J.* 16 (2010) 189–201.
- [42] I. Svorstol, H. Hoiland, J. Songstad, *Acta Chem. Scand. B: Org. Chem. Biochem.* 38 (1984) 885–893.
- [43] S. Balt, G. Duchattell, W. Dekieviet, A. Tieleman, *Z. Naturforsch. Sect. B* 33 (1978) 745–749.
- [44] J.A. Labinger, J.A. Osborn, N.J. Coville, *Inorg. Chem.* 19 (1980) 3236–3243.
- [45] G.P. Algra, S. Balt, *Inorg. Chem.* 20 (1981) 1102–1106.
- [46] G. Alibrandi, R. Romeo, L.M. Scolaro, M.L. Tobe, *Inorg. Chem.* 31 (1992) 5061–5066.
- [47] J.M. Fraile, J.I. Garcia, M.J. Gil, V. Martinez-Merino, J.A. Mayoral, L. Salvatella, *Chem. Eur. J.* 10 (2004) 758–765.
- [48] T. Hatakeyama, S. Hashimoto, K. Ishizuka, M. Nakamura, *J. Am. Chem. Soc.* 131 (2009) 11949–11963.
- [49] G. Kovacs, G. Ujaque, A. Lledós, *J. Am. Chem. Soc.* 130 (2008) 853–864.
- [50] M.S.W. Chan, K. Vanka, C.C. Pye, T. Ziegler, *Organometallics* 18 (1999) 4624–4636.
- [51] D. Braga, F. Grepioni, E. Tedesco, M.J. Calhorda, Z. Anorg. Allg. Chem. 626 (2000) 462–470.
- [52] I.E. Nifant'ev, L.Y. Ustynyuk, D.N. Laikov, *Organometallics* 20 (2001) 5375–5393.
- [53] P.G. Belelli, M.M. Branda, N.J. Castellani, *J. Mol. Catal. A* 192 (2003) 9–24.
- [54] I.E. Nifant'ev, L.Y. Ustynyuk, D.V. Besedin, *Organometallics* 22 (2003) 2619–2629.
- [55] E. Zurek, T. Ziegler, *Prog. Polym. Sci.* 29 (2004) 107–148.
- [56] T. Ziegler, K. Vanka, Z.T. Xu, C. R. Chim. 8 (2005) 1552–1565.
- [57] S.H. Yang, J. Huh, W.H. Jo, *Macromolecules* 38 (2005) 1402–1409.
- [58] J.M. Duceire, L. Cavallo, *Organometallics* 25 (2006) 1431–1433.
- [59] P.G. Belelli, N.J. Castellani, *J. Mol. Catal. A* 253 (2006) 52–61.
- [60] T.A. Manz, S. Sharma, K. Phomphrai, K.A. Novstrup, A.E. Fenwick, P.E. Fanwick, G.A. Medvedev, M.M. Abu-Omar, W.N. Delgass, K.T. Thomson, J.M. Caruthers, *Organometallics* 27 (2008) 5504–5520.
- [61] S. Tomasi, A. Razavi, T. Ziegler, *Organometallics* 28 (2009) 2609–2618.
- [62] J.R. Miecznikowski, S. Grundemann, M. Albrecht, C. Megret, E. Clot, J.W. Faller, O. Eisenstein, R.H. Crabtree, *Dalton Trans.* (2003) 831–838.
- [63] L.R. Moore, E.C. Western, R. Craciun, J.M. Spruell, D.A. Dixon, K.P. O'halloran, K.H. Shaughnessy, *Organometallics* 27 (2008) 576–593.
- [64] D. Zuccaccia, L. Belpassi, F. Tarantelli, A. Macchioni, *J. Am. Chem. Soc.* 131 (2009) 3170–3171.